Article

On the Moving of Neutral Point for Mn Subject to Submerged Arc Welding under Various Heat Inputs: Case Study into CaF$_2$-SiO$_2$-Na$_2$O-MnO Agglomerated Fluxes

Dan Zhang [1], Guoyou Shao [2], Jin Zhang [2,3,*] and Zhongqiu Liu [3]

[1] Department of Science and Technology, Suqian University, Suqian 223800, China
[2] School of Mechanical and Electrical Engineering, Suqian University, Suqian 223800, China
[3] School of Metallurgy, Northeastern University, Shenyang 110819, China
* Correspondence: 18142@squ.edu.cn

Abstract: Neutral Point indicates the flux formula where no transfer of alloying element between the flux and weld metal occurs. For the submerged arc welding process, Neutral Point is an essential definition for flux design and specification since it helps to identify the flux microalloying ability. The scientific hypothesis that the Neutral Point is only a function of the flux formula is considered as the basis of the Mitra kinetic model. Within this framework, by performing submerged arc welding with CaF$_2$-SiO$_2$-Na$_2$O-MnO agglomerated fluxes under various heat inputs, the moving of Neutral Point has been captured, indicating the scientific hypothesis proposed in Mitra kinetic model may be revised under high heat input welding. Additionally, although some studies have incorporated the consideration of the gas-slag-metal equilibrium, only the effective equilibrium temperature of 2000 or 2100 °C is utilized, which may be insufficient to constrain Mn content in the weld metal. In this study, we have incorporated all possible effective equilibrium temperatures that may be attained in the submerged arc welding process to simulate the transfer behavior of Mn. Then, a novel thermodynamic approach is proposed to detect the moving direction of Neutral Point for Mn from both slag-metal and gas-slag-metal equilibrium considerations, which may pave a vital way for the flux design and the setting of welding parameters. The factors responsible for the deviation between real and predicted data are discussed. The mechanism responsible for the moving of Neutral Point regarding the Mn element is evaluated from the perspective of both slag-metal and gas-slag-metal equilibrium considerations.

Keywords: neutral point; Calphad; submerged arc welding process; welding process simulation; thermodynamics

1. Introduction

In the process of submerged arc welding (SAW), an arc is maintained between the electrode and a blanket of granular flux which shields the hot weld metal (WM) and the arc from the atmosphere [1]. The high deposition rates obtained in such an automated welding process make it a very economical method of metal joining, especially in fields of heavy manufacturing industries.

During the SAW process, chemical reactions take place between arc plasma, weld pool, and the (flux) slag (flux means the starting material before welding, while slag implies the molten or solidified flux during or after welding); the complicated chemical interactions result in compositional changes of the metal, which further dictates the mechanical properties of the weldment [2]. Therefore, it is necessary to control the WM composition properly to ensure a sound weld.

One of the primary concerns in WM composition control is to design and select fluxes; this requirement would be better fulfilled with further understanding of the elemental transfer behavior in the SAW process [3]. Generally, the final WM composition for a

particular element is made up of the contributions from the electrode, base metal (BM), and that transfer between flux and WM [1,4]. The compositional contribution from the electrode and the BM is quantified by a nominal composition, indicating the compositional contributed from the simple mixing of the electrode and BM in the absence of chemical reactions [5,6]. The extent of loss or gain of a specific element between flux and WM is quantified by a Δ value, which is the difference between the analytical and nominal composition. A positive Δ value indicates an elemental gain from the flux, whereas a negative Δ value indicates an elemental loss from WM to the slag [4,7].

To better describe the element transfer behavior between flux and WM, Chai and Eagar et al. [6,8–10] have proposed a "Neutral Point" (*NP*) definition to describe the flux formula where no transfer of alloying element between the flux and WM. *NP* definition is important for flux design and selection since it dictates the microalloying ability of flux for the WM.

Based on the assumed slag-metal equilibrium attained in SAW, Mitra et al.[7,11–13] concluded that the *NP* is only a function of the flux formula and is not affected by the variations of the SAW parameters; this conclusion is of critical importance since it is the basis for Mitra et al. [11,13] to develop the kinetic model. However, it is noted that the SAW experiments performed by Chai and Mitra et al. [8,13] were under heat input of 20 kJ/cm due to technical limitations in early trials. Recently, to further improve welding efficiency, SAW with higher heat input has been widely applied [2,14–16].

As for SAW, one may propose that the extremely high temperature and surface-to-volume ratios could allow for thermodynamic equilibrium to be attained locally; as such, knowledge of thermodynamic equilibrium could be employed to constrain chemical reactions and mechanisms involved in the welding process [3,4,17]. Since the arc plasma, molten slag, and weld pool are shielded under the flux, it is impossible to measure the real temperature in the SAW process [2]. To encounter this difficulties, a definition of "effective equilibrium temperature" (EET) has been proposed to aid in thermodynamic calculation; EET does not imply the measured temperature but indicates the temperature at which the experimental mass action index equals the equilibrium constant [2]. Researchers have proposed different EET values subject to SAW, as summarized in Table 1.

Table 1. EET values concluded by different investigators (°C).

Researchers	Proposed EETs
Chai et al. [8]	2000
S. Liu et al. [3]	1900
Coetsee et al. [18]	2100
Mitra et al. [19]	1700 to 2000
Belton et al. [20]	1930 to 2030
Christensen et al. [21]	1800 to 2100

As mentioned previously, although the real EET is unmeasurable technically, recent studies indicate the level of EET generally increases with higher heat input [14,15,22]. Considering the improvement in heat input may influence the value of EET and the transfer behavior of Mn, we are poised to design CaF_2-SiO_2-Na_2O-MnO agglomerated fluxes with varying MnO contents and locate the *NPs* of fluxes for Mn under different heat input.

Transfer behavior of Mn is the primary concern within this framework due to that:

1. Mn is an important acicular ferrite (AF) promotion element for the WM. It has been well established that the increasing Mn level from 0.6 to 1.8 wt pct could gradually improve the AF fraction [2,23].
2. The decomposition of MnO, as well as the evaporation of Mn from the weld pool, tend to affect the transfer behavior of Mn; however, such factors were not considered when the *NP* definition is proposed.

The present study has been undertaken to investigate the moving mechanism of *NP* point for Mn subject to various heat inputs of 20 and 60 kJ/cm. The moving behavior of *NP* is quantified and interpreted from both slag-metal and gas-slag-metal equilibrium considerations via Calphad technology. By analyzing the thermodynamic and real data, attempts are made to propose modification suggestions for *NP* definition subject to various heat inputs in the SAW process.

2. Materials and Methods

2.1. Flux and Metal Preparation

For each flux recipe, reagent-grade powders were mixed in a blender at 0.5 Hz for half an hour. Then, the powders were bonded by the sodium-silicate solution. The bonded mixtures were pelletized and dried in the muffle furnace at 600 °C for 3 h. At last, the mixtures were broken up and screened to 14 to 100 mesh. X-ray fluorescence was employed to determine the compositions of fluxes. Since it is well known that all Mn-oxides decompose to MnO above 530 °C, MnO is reported as part of the flux compositions. The analytical flux composition is given in Table 2. As shown in Table 2, the compositional change in Na_2O and SiO_2 is neglectable, and the MnO level improves from 0 to 60 wt pct gradually, with CaF_2 making up the remainder. The basicity index (*BI*) of each flux is determined by Equation (1) (wt pct).

$$BI = \frac{CaO + CaF_2 + MgO + Na_2O + K_2O + 0.5 \times (MnO + FeO)}{SiO_2 + 1/2(Al_2O_3 + Cr_2O_3 + TiO_2 + ZrO_2)} \tag{1}$$

Table 2. Measured compositions of fluxes (wt pct).

Fluxes	CaF_2	Na_2O	SiO_2	MnO	*BI*	Predicted O from *BI* Model
F-0	60.08	1.23	38.69	0	1.58	0.029
F-1	48.40	1.24	40.15	10.21	1.36	0.032
F-2	36.79	1.21	41.22	20.78	1.17	0.035
F-3	29.50	1.19	39.45	29.86	1.16	0.036
F-4	18.89	1.31	38.68	41.12	1.05	0.040
F-5	10.15	1.18	38.13	50.54	0.96	0.041
F-6	0	1.29	40.53	58.18	0.75	0.056

2.2. Welding Experiment

Typical low alloy steel, Q345A, was selected as base metal (BM). Bead-on-plate double-electrodes single-pass SAW was performed at heat input of 60 kJ/cm (DC-850 A/32 V for electrode forward, AC-625 A/36 V for electrode backward, 500 mm/min) and 20 kJ/cm (DC-436 A/30 V, 393 mm/min), respectively. Inductively coupled plasma optical emission spectrometry (ICP-OES) was used to determine metallic element content, while LECO analyzer was used to determine O contents. Compositions of the electrode and BM are given in Table 3.

Table 3. Measured chemical compositions of BM and electrode (wt pct).

	C	Si	Mn	Ti	Al	O
BM(Q345A)	0.113	0.142	1.540	0.01	0.12	0.003
Electrode	0.127	0.138	1.650	0.01	0.14	0.003

2.3. Thermodynamic Calculation

2.3.1. The MnO Activity in Flux

FactSage Equilib module was utilized to calculate the activity of MnO:

1. FToxid, Fstel, and FactPS databases are selected. Solution phases of ASlag-liq all oxides, S (FToxid-SLAGA) were selected to model the molten slag.

2. The equilibrium temperatures of 1700, 1800, 1900, 2000, and 2100 °C were set. The setting temperatures are based on the reported EET value in Table 1.

Measured flux compositions in Table 2 were set as input.
The calculated activities are given in Table 4.

Table 4. Calculated MnO activity under various EET.

EET	F-0	F-1	F-2	F-3	F-4	F-5	F-6
1700	0	0.043	0.073	0.106	0.149	0.184	0.194
1800	0	0.052	0.088	0.125	0.171	0.209	0.220
1900	0	0.061	0.103	0.145	0.194	0.234	0.247
2000	0	0.072	0.119	0.164	0.217	0.258	0.273
2100	0	0.082	0.136	0.184	0.238	0.281	0.298

2.3.2. Gas-Slag-Metal Equilibrium Calculation

FactSage Equilib module of FactSage was employed to perform gas-slag-metal equilibrium calculation:

1. FToxid, Fstel, and FactPS databases were selected. Solution phases of ASlag-liq all oxides, S (FToxid-SLAGA), and LIQUID (FStel-Liqu) were selected to model the molten slag and steel phases.
2. The equilibrium temperatures of 1700, 1800, 1900, 2000, and 2100 °C were set.
3. Nominal compositions were used as the input metal chemistries. Measured flux compositions in Table 2 were set as flux input.
4. Since the differences between BM and electrode compositions are small, the nominal composition was set as average compositions of electrode and BM.

3. Results and Discussion

3.1. Moving of NP Subject to Slag-Metal Equilibrium Consideration

The assumption that *NP* is only a function of the flux formula has been proposed on the basis of the slag-metal equilibrium consideration in SAW [10]. The slag-metal equilibrium model was developed by Chai et al. [8,9] based on the following assumptions:

1. An empirical relationship exists between flux *BI* flux and the WM O content (see Figure A1 in Appendix A). In another word, the WM O content is only a function of flux formula.
2. The EET of chemical reactions holds constant at 2000 °C.
3. The activity data is extrapolated to 2000 °C by applying acceptable models (regular solution model).
4. The transfer of Mn is controlled by Reaction (2) at the slag-metal interface. The content of Mn is then calculated from the predicted WM O content, MnO activity, and equilibrium constant of Reactions (2), as shown by Reaction (3).

$$(MnO) = [Mn] + [O] \tag{2}$$

$$[pct\ Mn] = \frac{\alpha_{MnO}}{0.86 \cdot [pct\ O]} \tag{3}$$

The O content predicted by the *BI* model is given in Table 2. It is noted that the *BI* model is rendered semi-empirical since it was developed on the measured data and flux formula [24]. However, extensive studies have demonstrated that the heat input of SAW exert a significant impact on the level of flux O potential [14,15,25].

As mentioned previously, there are no technical means to measure and determine the real equilibrium temperature of SAW. Nonetheless, the thermodynamic analysis, coupled with the heat source simulation, demonstrated that the EET generally increases with higher heat input [14,15,22]. With this in mind, the Mn content is predicted from the predicted

O content and MnO activity under various EETs (see Table 2) by using the slag-metal equilibrium model (Reaction(3)) with the predicted data plotted in Figure 1.
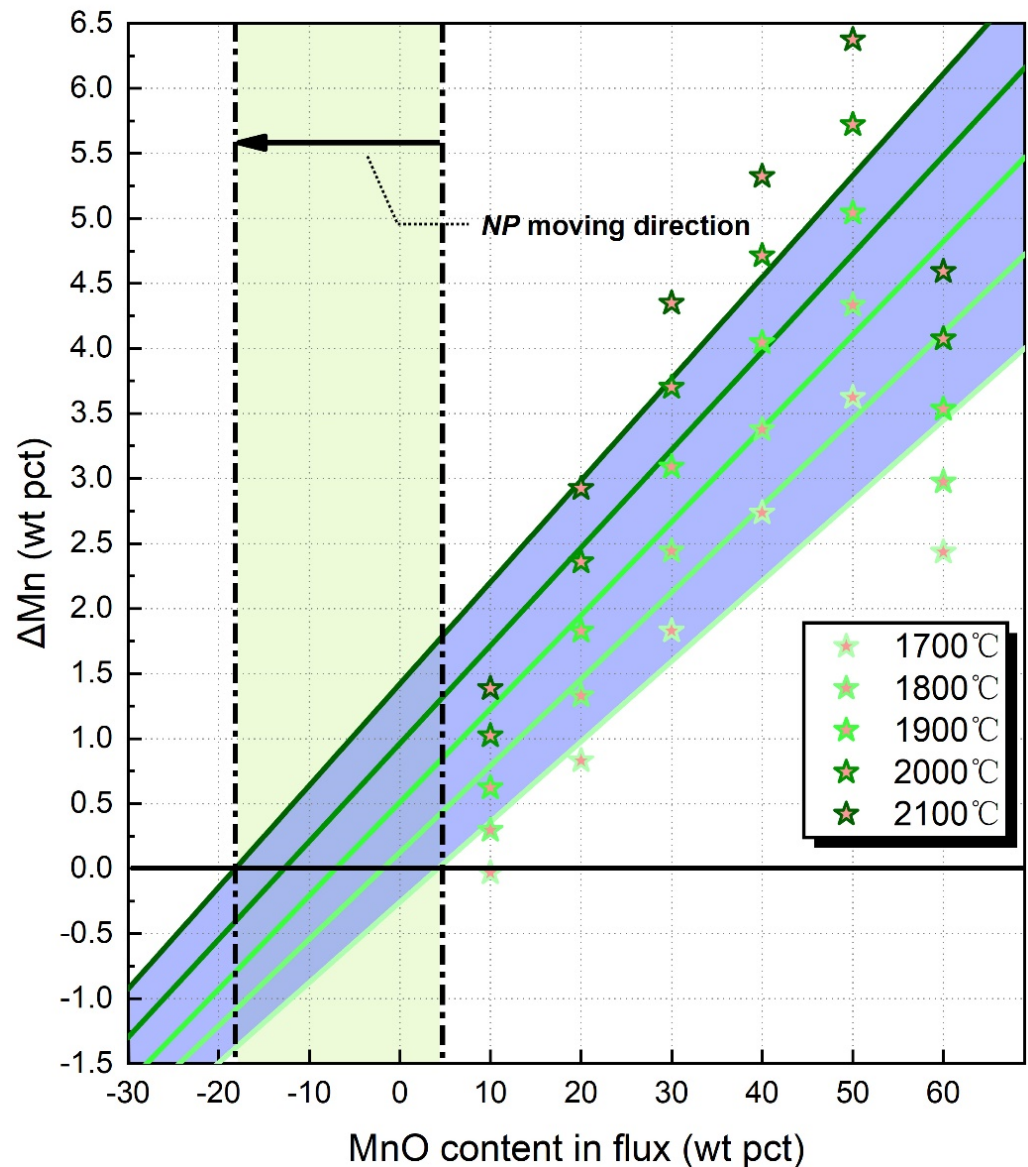

Figure 1. The *NPs* calculated by slag-metal equilibrium model: the star-points indicate the predicted ΔMn values subject to various EET.

Based on the ΔMn values in Figure 1, we located the *NPs* subject to different heat inputs following the method stated elsewhere [13]. As shown by the black arrow, *NP* moves from 4 to −18 wt pct MnO when the EET increases from 1700 to 2100 °C.

3.2. Moving of NP Subject to Gas-Slag-Metal Equilibrium Consideration

It is well known that there are essential shortcomings concerning the slag-metal equilibrium model, although this model is considered as the foundation for the definition of *NP* [2,26].

1. The slag-metal equilibrium model relies on the empirical *BI* model to predict O content. A major concern of the *BI* model is that the predicted O content is only dependent on the flux formula.
2. The slag-metal equilibrium model only considers the activity of MnO in the initial flux (not in slag).

3. Although it is well known in SAW engineering that the significant Mn evaporation tends to occur during the welding process, such effect on the transfer of Mn is not considered.

Recently, thermodynamic databases for gases, oxides, and alloy systems have been developed by the Calphad technique; based on the applicable models (such as the cell model and modified regular solution model), the thermodynamic data could be extrapolated to higher temperatures, even higher than 2000 °C [27,28]. The ΔMn values calculated by the gas-slag-metal equilibrium model are illustrated in Figure 2. The *NP*s subject to different heat inputs are then located. It can be seen that *NP* moves from 10 to −2 wt pct MnO when the EET increases from 1700 to 2100 °C.
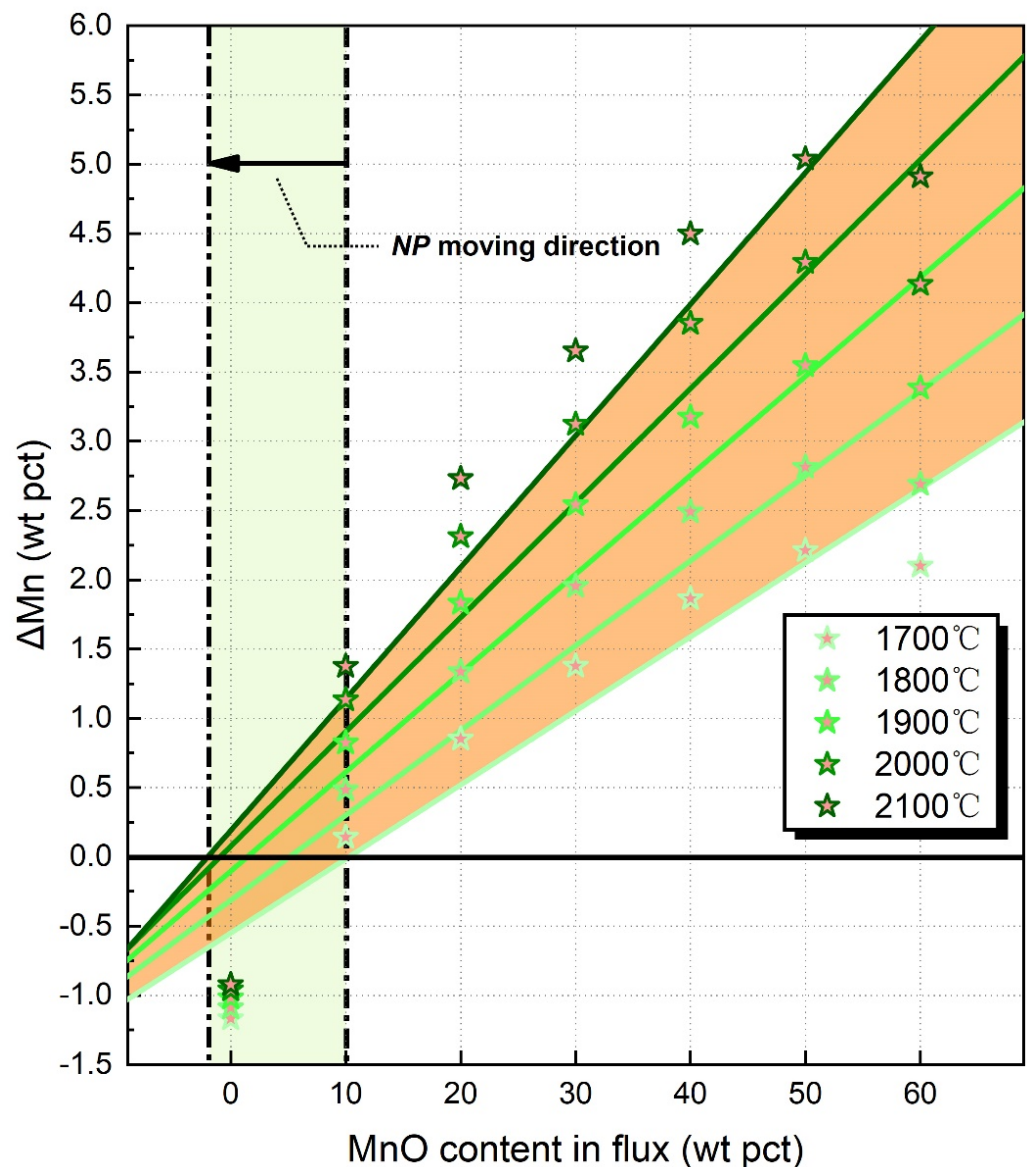

Figure 2. The *NP*s calculated by slag-metal equilibrium model: the star-points indicate the predicted ΔMn values subject to various EET.

3.3. Deviation between Real and Predicted NPs

The real ΔMn data, coupled with the corresponding *NP*s, are plotted in Figure 3. In Figure 3, the blue shaded area indicates the ΔMn zone precited by slag-metal equilibrium, the orange shaded area indicates the ΔMn zone precited by gas-slag-metal equilibrium, the red shaded area indicates the real ΔMn zone. It is seen that when the heat input increases

from 20 to 60 kJ/cm, the *NP* moves from 20 to 10 wt pct MnO. Based on observation from Figures 1–3, it is concluded that both slag-metal and gas-slag-metal equilibrium models are capable of predicting the moving direction of *NP* for Mn with higher heat input.
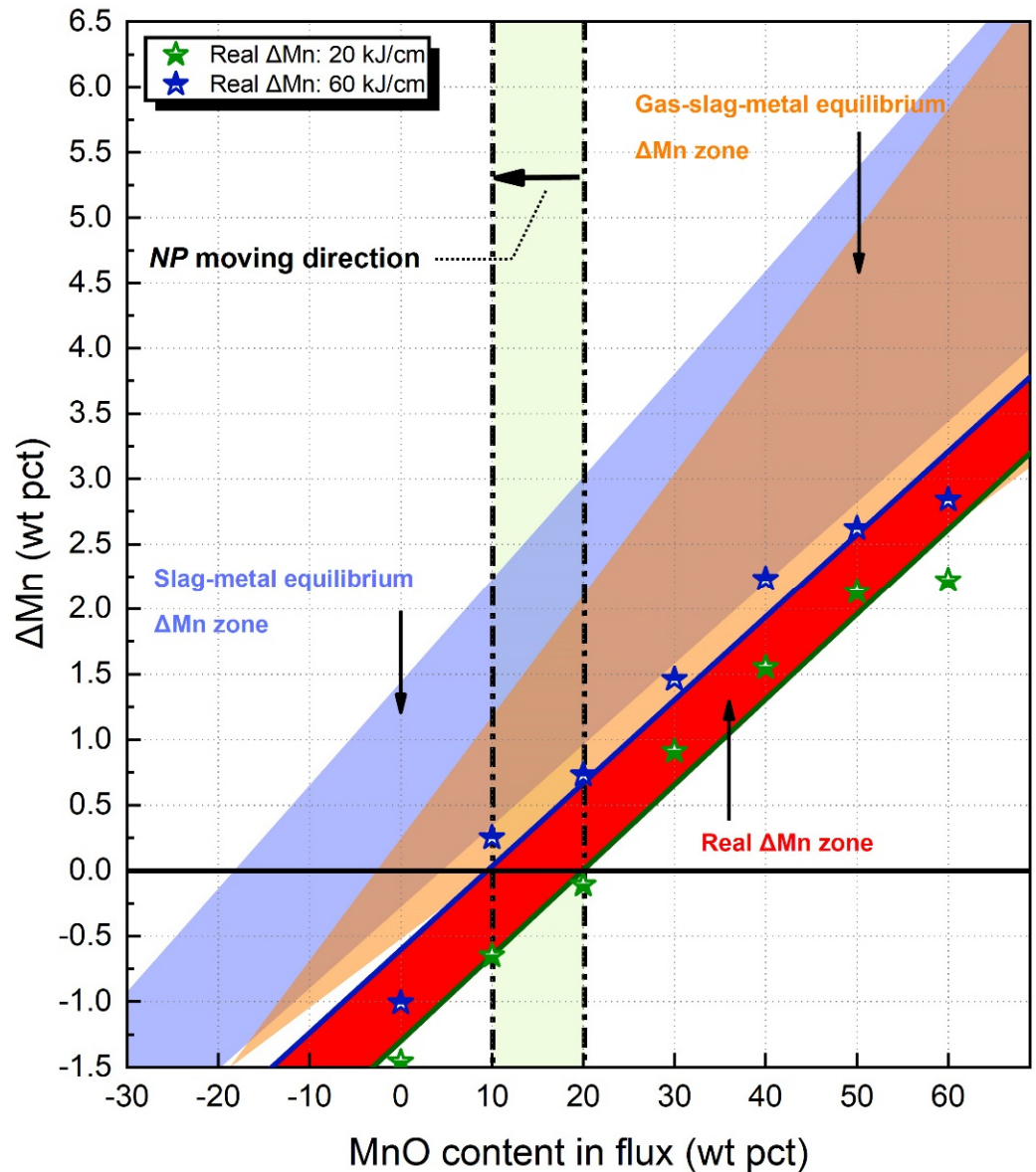

Figure 3. The real *NPs* calculated as a function of MnO content in flux.

Furthermore, the shaded areas in Figure 3 indicate that the ΔMn predicted by the gas-slag-metal equilibrium model is closer to the reals ones in comparison to those predicted by the slag-metal equilibrium model. Three factors may be responsible for the deviation between real and predicted data:

1. Prediction for WM O content (flux O potential).
2. Prediction for MnO activity.
3. Whether the loss of Mn from evaporation is considered.

To further evaluate the deviation between real and predicted data, the essential thermodynamic data pertinent to the transfer behavior of Mn is given in Figure 4a–f.
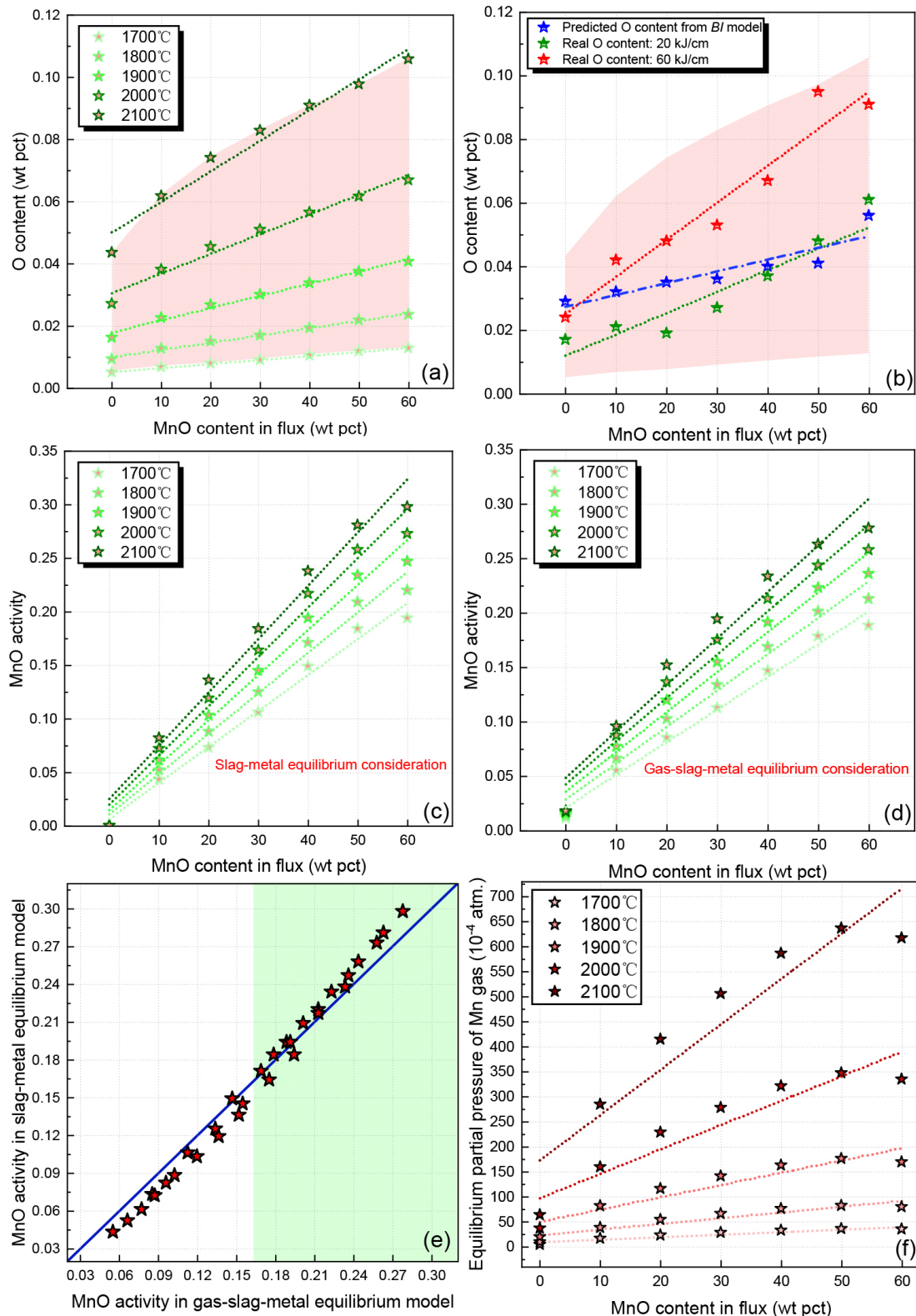
Figure 4. Essential thermodynamic data pertinent to the transfer behavior of Mn: (**a**) predicted O content subject to various EET from gas-slag-metal equilibrium model, (**b**) Real O content of the WM and that predicted from slag-metal equilibrium model (the *BI* model), (**c**) MnO activity in slag-metal and slag-metal equilibrium model, (**d**) MnO activity in gas-slag-metal and slag-metal equilibrium model, (**e**) deviants between simulated MnO activities in flux and slag, (**f**) Level of equilibrium partial pressure of Mn.

3.3.1. Prediction for WM O Content (Flux O Potential)

Figure 4a illustrates the predicted O content subject to various EET from the gas-slag-metal equilibrium model. The red shaded area in Figure 4a provides a zone for the possible O content in the WM subject to different heat inputs. Figure 4b illustrates the real O content of the WM and that predicted from the slag-metal equilibrium model (the *BI* model). The red and green star-points in Figure 4b show that the gas-slag-metal equilibrium model can place constraint on the O content, even under different heat input. Additionally, as shown in Figure 4a,b, the WM O content (flux O potential) increases with higher heat input for a given flux formula, that is, higher heat input exsert a synergism effect on the flux O potential, which is in agreement with the measured data reported in previous studies [15,25]. The slag-metal equilibrium model (the *BI* model), on the other hand, did not consider the impact of heat input on the flux O potential, as shown by the blue start-points in Figure 4b.

3.3.2. Prediction for MnO Activity

According to Equation (3), MnO is an essential factor governing the transfer behavior of Mn in addition to WM O content. The employed MnO activity in both slag-metal and gas-slag-metal equilibrium models have been plotted in Figure 4c,d. By comparing the level of O content and MnO activity in Figure 4a–d, the absolute value of MnO activity is one order higher than that of O content. Therefore, it is concluded that the level of MnO activity is the major factor convening the changing trend of ΔMn as a function of the flux formula, which can be reflected by the green lines illustrated in Figures 1, 2 and 4c,d.

Additionally, the slag-metal model only considered the MnO activity in initial flux. However, the complicated chemical reactions in SAW process would induce the compositional change between flux and slag, which, in turn, dictates the MnO activity [26,29]. On the other hand, the gas-slag-metal equilibrium model developed via Calphad technology performed the thermodynamic calculation using the MnO activity in the molten slag [28]. The differences between simulated MnO activities in flux and slag are plotted in Figure 4e. It is seen from Figure 4e that, at the range of MnO activity, the MnO activity is overestimated by the slag-metal equilibrium model.

3.3.3. Mn Loss from the SAW System Due to Evaporation

Significant reduction in Mn via evaporation during the SAW process has been extensively confirmed; however, such loss is not considered in the slag-metal equilibrium model [19,26,30,31]. The level of equilibrium partial pressure of Mn is given in Figure 4f, indicating the gas-slag-metal equilibrium model is able to predict the evaporation behavior of the Mn element in the welding process. It is noted that the sole consideration of thermodynamics is insufficient to predict the evaporation of Mn accurately [26]. Actually, different models have been proposed to predict the level of Mn loss via evaporation during arc welding, although these approaches invariably overpredict the data by a factor of 10 or more [31]. A deeper understanding with respect to the nature of the arc plasma is anticipated to further improve the prediction accuracy for Mn transfer behaviors in SAW [2].

Therefore, the gas-slag-metal equilibrium model predicted the *NP* for Mn transfer with higher accuracy than the slag-metal equilibrium model for the following reasons:

1. The gas-slag-metal equilibrium model is capable of constraining the level of WM O content under different EETs (heat input). Slag-metal equilibrium model, on the other hand, only considers the impact of flux formula on WM O content.
2. The slag-metal equilibrium model may overestimate the MnO activity in the initial flux at a higher level of activity level since the compositional change between flux and slag is not considered.
3. The slag-metal equilibrium model only considers the slag-metal reaction with respect to Mn transfer, whereas the gas-slag-metal equilibrium model could constrain the loss of Mn due to evaporation in the SAW process.

In SAW engineering, the Mn content refers to the chemistry in the bulk metal (not at the interface). The Mn transfer (the distribution of Mn in the cross-section) has been reported previously [11,19]. In the region zone of cooling and solidifying the weld pool, the molten weld pool behind the electrode starts to cool as the electrode moves away. It was found that there is a small drop in the Mn content near the slag-metal interface, which is attributed to the increasing stability of oxides at lower temperatures and the consequent shifting of Reaction (2) to the left side [11,19].

Additionally, the SiO_2 level is held constant due to the SiO_2 being the network-builder of the slag, and the changing of the SiO_2 level would make the welding process unstable [14]. Additionally, other reactions among the flux compounds (e.g., dissociation of SiO_2) and influence on Mn have been considered by the FactSage Equilib module [28].

4. Conclusions

Within this framework, CaF_2-SiO_2-Na_2O-MnO agglomerated fluxes with varying MnO levels are designed and applied to submerged arc welding subject to different heat inputs of 20 and 60 kJ/cm. The major findings of this investigation are as follows:

1. When heat input improves from 20 to 60 kJ/cm, the *NP* of Mn moves from 20 to 10 wt pct MnO.
2. By utilizing the possible EETs that may be attained in the SAW process, it is revealed that both slag-metal and gas-slag-metal equilibrium models are capable of predicting the moving direction of *NP* for Mn transfer, which may aid in the flux design and the setting of welding parameters.
3. The ΔMn is overestimated by the slag-metal equilibrium model since the loss of Mn due to evaporation is not considered. When the gas-slag-metal equilibrium model is employed, the prediction accuracy for the *NP* is improved.
4. By analyzing the measured and thermodynamic data, it is concluded that the moving of the *NP* is primarily attributed to the improvement of EET with higher heat input.
5. The scientific hypothesis that *NP* is only a function of the flux formula (one of the essential bases for the Mitra kinetic mode) may be revised since the transfer behavior of the alloying element is essentially controlled by complex thermodynamic factors, especially the value of EET. The consideration of heat input may be needed to further improve the prediction accuracy of the Mitra kinetic model, which will be reported in our coming work.
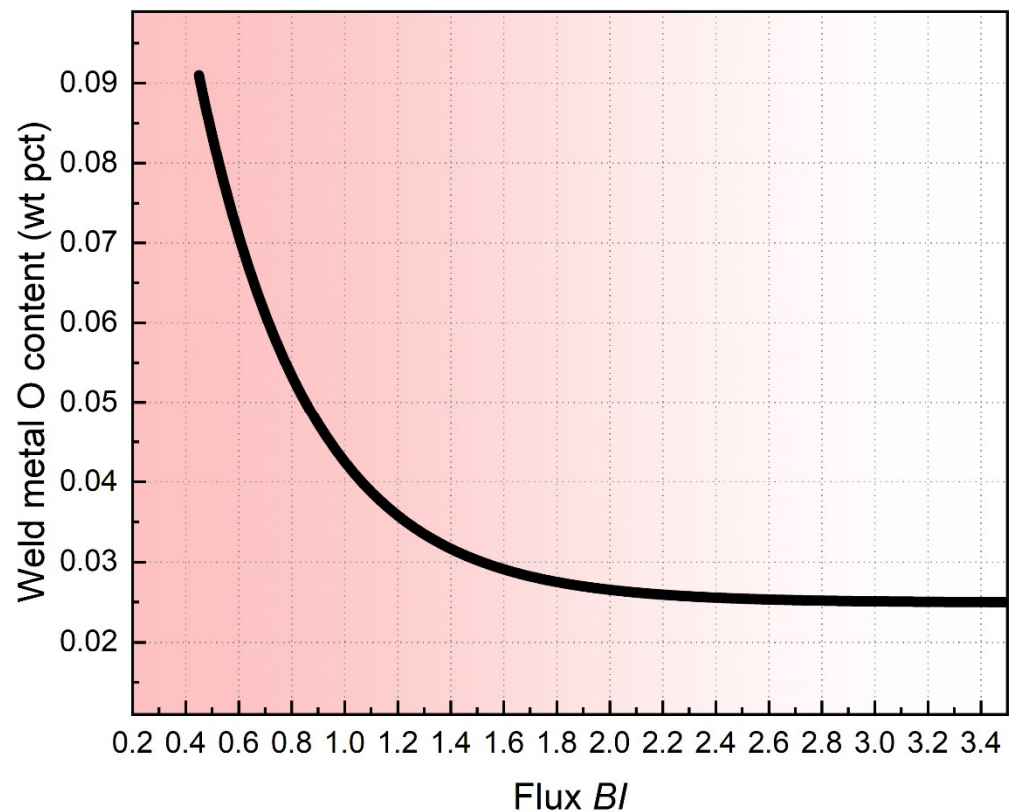
Appendix A Flux *BI* Model

Figure A1. WM O content as a function of flux *BI* value [24].

References

1. Sengupta, V.; Havrylov, D.; Mendez, P. Physical Phenomena in the Weld Zone of Submerged Arc Welding-A Review. *Weld. J.* **2019**, *98*, 98–283. [CrossRef]
2. Cong, W.; Zhang, J. Fine-tuning Weld Metal Compositions via Flux Optimization in Submerged Arc Welding: An Overview. *Acta Metall. Sin.* **2022**, *57*, 1126–1140. [CrossRef]
3. Olson, D.; Liu, S.; Frost, R.; Edwards, G.; Fleming, D. Nature and Behavior of Fluxes Used for Welding. In *ASM Handbook*; ASM International: Almere, Netherlands, 1993; Volume 6, pp. 55–63. [CrossRef]
4. Natalie, C.A.; Olson, D.L.; Blander, M. Physical and Chemical Behavior of Welding Fluxes. *Annu. Rev. Mater. Sci.* **1986**, *16*, 389–413. [CrossRef]
5. Kanjilal, P.; Pal, T.; Majumdar, S. Prediction of Element Transfer in Submerged Arc Welding. *Weld. J.* **2007**, *10*, 40.
6. Chai, C.; Eagar, T. Prediction of Weld-metal Composition during Flux-shielded Welding. *J. Mater. Energy Syst.* **1983**, *5*, 160–164. [CrossRef]
7. Mitra, U.; Eagar, T. Slag-metal reactions during welding: Part I. Evaluation and Reassessment of Existing Theories. *Metall. Trans. B* **1991**, *22*, 65–71. [CrossRef]
8. Chai, C.; Eagar, T. Slag-Metal Equilibrium during Submerged Arc Welding. *Metall. Trans. B* **1981**, *12*, 539–547. [CrossRef]
9. Chai, C.-S. Slag-metal Reactions during Flux Shielded Arc Welding. Ph.D. Thesis, Massachusetts Institute of Technology, Cambridge, MA, USA, 1980.
10. Eagar, T.W. Thermochemistry of joining. In Proceedings of the Elliott Symposium on Chemical Process Metallurgy, Cambridge, MA, USA, 10–13 June 1990.
11. Mitra, U.; Eagar, T. Slag-metal Reactions During Welding: Part II. Theory. *Metall. Trans. B* **1991**, *22*, 73–81. [CrossRef]
12. Mitra, U.; Eagar, T. Slag-metal Reactions during Welding: Part III. Verification of the Theory. *Metall. Trans. B* **1991**, *22*, 83–100. [CrossRef]
13. Mitra, U. *Kinetics of Slag Metal Reactions during Submerged Arc Welding of Steel*; Massachusetts Institute of Technology: Cambridge, MA, USA, 1984.
14. Zhang, J.; Coetsee, T.; Wang, C. Element Transfer Behaviors of Fused CaF_2-SiO_2 Fluxes Subject to High Heat Input Submerged Arc Welding. *Metall. Mater. Trans. B* **2020**, *51*, 16–21. [CrossRef]
15. Zhang, J.; Coetsee, T.; Dong, H.; Wang, C. Element Transfer Behaviors of Fused CaF_2-SiO_2-MnO Fluxes under High Heat Input Submerged Arc Welding. *Metall. Mater. Trans. B* **2020**, *51*, 885–890. [CrossRef]

16. Zhang, J.; Leng, J.; Wang, C. Tuning Weld Metal Mechanical Responses via Welding Flux Optimization of TiO$_2$ Content: Application into EH36 Shipbuilding Steel. *Metall. Mater. Trans. B* **2019**, *50*, 2083–2087. [CrossRef]
17. Indacochea, J.E.; Blander, M.; Christensen, N.; Olson, D.L. Chemical Reactions During Submerged Arc Welding with FeO-MnO-SiO$_2$ Fluxes. *Metall. Trans. B* **1985**, *16*, 237–245. [CrossRef]
18. Coetsee, T.; Mostert, R.J.; Pistorius, P.G.H.; Pistorius, P.C. The Effect of Flux Chemistry on Element Transfer in Submerged Arc Welding: Application of Thermochemical Modelling. *J. Mater. Res. Technol.* **2021**, *11*, 2021–2036. [CrossRef]
19. Mitra, U.; Eagar, T. Slag Metal Reactions During Submerged Arc Welding of Alloy Steels. *Metall. Trans. A* **1984**, *15*, 217–227. [CrossRef]
20. Belton, G.; Moore, T.; Tankins, E. Slag-metal Reactions in Submerged Arc Welding. *Weld. J.* **1963**, *42*, 289s–297s.
21. Christensen, N.; Chipman, J. Slag-metal interaction in arc welding. *Weld. J.* **1953**, *15*, 1–14.
22. Gery, D.; Long, H.; Maropoulos, P. Effects of Welding Speed, Energy Input and Heat Source Distribution on Temperature Variations in Butt Joint Welding. *J. Mater. Process. Technol.* **2005**, *167*, 393–401. [CrossRef]
23. Ricks, R.; Howell, P.; Barritte, G. The nature of acicular ferrite in HSLA steel weld metals. *J. Mater. Sci.* **1982**, *17*, 732–740. [CrossRef]
24. Tuliani, S.; Boniszewski, T.; Eaton, N. Notch Toughness of Commercial Submerged Arc Weld metal. *Weld. Met. Fabr.* **1969**, *37*, 327–339.
25. Dallam, C.; Liu, S.; Olson, D. Flux Composition Dependence of Microstructure and Toughness of Submerged Arc HSLA Weldments. *Weld. J.* **1985**, *64*, 140–151.
26. Zhang, J.; Wang, C.; Coetsee, T. Assessment of Weld Metal Compositional Prediction Models Geared Towards Submerged Arc Welding: Case Studies Involving CaF$_2$-SiO$_2$-MnO and CaO-SiO$_2$-MnO Fluxes. *Mater. Trans. B* **2021**, *52*, 2404–2415. [CrossRef]
27. Jung, I.-H. Overview of the Applications of Thermodynamic Databases to Steelmaking Processes. *Calphad* **2010**, *34*, 332–362. [CrossRef]
28. Bale, C.W.; Bélisle, E.; Chartrand, P.; Decterov, S.; Eriksson, G.; Gheribi, A.; Hack, K.; Jung, I.-H.; Kang, Y.-B.; Melançon, J. Reprint of: FactSage Thermochemical Software and Databases, 2010–2016. *Calphad* **2016**, *55*, 1–19. [CrossRef]
29. Zhang, J.; Wang, C.; Coetsee, T. Thermodynamic Evaluation of Element Transfer Behaviors for Fused CaO-SiO$_2$-MnO Fluxes Subjected to High Heat Input Submerged Arc Welding. *Metall. Mater. Trans. B* **2021**, *52*, 1937–1944. [CrossRef]
30. Lau, T.; Weatherly, G.; McLean, A. Gas/metal/slag Reactions in Submerged Arc Welding Using CaO-Al$_2$O$_3$ Based Fluxes. *Weld. J.* **1986**, *65*, 31–38.
31. Kou, S. *Welding Metallurgy*, 3rd ed.; JohnWiley & Sons, Inc.: Hoboken, NJ, USA, 2003; pp. 22–122.